



Synthesis and Evaluation of New Poly Cationic Surfactants as Corrosion Inhibitors for Carbon Steel in Formation Water

Amira E. El-Tabey¹, Ahmed G. Bedir^{1*}, E. A. Khamis¹, M. Abd-El-Raouf¹,
 Fouad Zahran^{2,3}, M. Adel Yousef², A. M. Al-Sabbagh¹

¹Egyptian Petroleum Research Institute (EPRI), Nasr City, Cairo, Egypt.

²Faculty of Science, Helwan University, Helwan, Cairo, Egypt.

³Helwan Nanotechnology Center, Helwan University, 11795, Helwan, Cairo, Egypt.



TWO new polycationic surfactants abbreviated as (PTEAA.10 and PTEAA.12) were prepared by homopolymerization of triethanolamine acrylate monomer followed by quaternization with 1-bromodecane and 1-bromododecane. FT-IR, ¹H-¹³CNMR, and GPC have been used to confirm the chemical structure of the prepared surfactants.

The prepared polycationic surfactants have been tested as corrosion inhibitors for carbon steel X65 in formation water. Weight loss, electrochemical impedance spectroscopy (EIS), and potentiodynamic polarization accompanied by SEM and EDX techniques were used to study the inhibition performance of PTEAA.10 and PTEAA.12. The prepared polymeric cationic surfactants act as mixed type inhibitors according to Tafel data. The inhibition efficiency of PTEAA.12 at 250 ppm was 92.8 %. The inhibition action was attributed to the formation of the adsorbed layer of surfactants over X65 surface that was follow Langmuir adsorption isotherm. The resistance of the adsorbed layer (R_{ct}) was a function in concentration and hydrophobicity of the surfactants.

Keywords: Corrosion inhibitor, EIS, Formation water, Langmuir adsorption isotherm, Poly cationic surfactant, SEM, Tafel.

Introduction

Corrosion is a complex process involving coupled chemical, electrochemical, biological, and solid state reaction dynamics, materials science, surface science, and environmental chemistry. The multiscale nature of corrosion processes and the need to connect across the length (and time) scales to advance our knowledge of the factors governing corrosion are daunting [1, 2].

Corrosion is fated but can be controlled via several ways such as cathodic protection, metal coatings, and corrosion inhibitors. The latter has been considered as the most effective, and easily applicable way [3, 4]. Carbon steel (X65) is the main constructive material in the gas-oil

industry due to its cost-effectiveness and excellent mechanical properties [5, 6]. The corrosiveness behavior of formation water comes from the presence of large quantities of the corrosive carbon dioxide and hydrogen sulfide in addition to other aggressive salts such as chloride and sulfate. The formation of water also contains traces of oxygen that could enter into the sour brine system [7, 8].

Formation water (produced water, oilfield brine, oilfield waste water or connate water) is water that occurs in association with oil and gas in reservoir rocks and is present in the rocks immediately before drilling. Most oil field water contains a variety of dissolved organic and inorganic compounds. The major elements

*Corresponding author e-mail: ahmedgamalepri@gmail.com

Received 1/4/2019; Accepted 21/7/2019

DOI: 10.21608/ejchem.2019.11344.1730

© 2020 National Information and Documentation Center (NIDOC)

usually present are sodium, calcium, magnesium, chloride, bicarbonate, and sulfate. Because of aggressive properties of the formation water, inhibitors are commonly used [9-12].

The use of organic compounds as corrosion inhibitors, which usually contain polar functional groups such as nitrogen, sulfur and oxygen heteroatoms remains the most economical practice for protection of carbon steel pipelines which exposed to oilfield brines. These corrosion inhibitors are believed to form self-assembled films that protect the steel surface against corrosion [13-16]. The synthesis of tailor-made polymeric surfactants has been gained a considerable interest that offers a more significant opportunity in terms of flexibility and functionality [17-19]. The application of surfactants as corrosion inhibitors has been studied by some authors [20-23].

Cationic surfactants, which are most relevant to the present study, usually fall into one of the following categories: long-chain amines or polyamines and their quaternized derivatives. Moreover, Aliphatic and aromatic amines, mono-, di-, or polyamines and their salts, all are used as corrosion inhibitors [24-26]. Using of polymeric cationic surfactants as corrosion inhibitors still need more studies, so this study focused on the preparation a new polymeric cationic surfactant based on triethanolamine acrylate monomer to increase the active sites along the polymer chain which are responsible for adsorption on the metal surface together with long hydrophobic polymer chains which act as a barrier against the corrosive medium. In this work, chemical structure of the synthesized polymeric surfactant was justified by GPC, FT-IR and HNMR spectroscopy. Moreover, the polymeric surfactants were evaluated as

a corrosion inhibitor using three techniques (Weight loss, Potentiodynamic polarization, and Electrochemical impedance).

Experimental Techniques and Materials

Materials

Triethanolamine (TEA) and acrylic acid (AA) were purchased from (Aldrich); 1-bromodecane and 1-bromododecane were purchased from (Merck-Germany). The solvents were used as received; they were all of the analytical grades. A polymerization inhibitor was added (hydroquinone) at 200 ppm to prevent robust exothermic polymerization of AA when exposed to light or heat.

Carbon steel

X65 carbon steel with chemical composition in wt. % (0.06 Si, 0.7 Mn, 0.001 S, 0.005 P, 0.016 Cr, 0.013Ni, 0.004 Mo, 0.06 C and Fe balanced).

Formation water

The typical formation water used in this study was collected from Qarun Petroleum Company, labeled (NED-1)-water source - Egypt (QPC) water. Its physical and chemical compositions are represented in Table 1.

Synthesis of the inhibitors

Synthesis of 2-(bis(2-hydroxy) amino) ethyl acrylate monoester

Triethanolamine (0.1 mol) and acrylic acid (0.1) were esterified in the presence of xylene as a solvent and 0.01% P-TSA (para-toluene sulfonic acid) as a catalyst and HQ (hydroquinone) as an inhibitor, until the azeotropic amount of water was collected. The prepared monoester -(2-(bis(2-hydroxy) amino) ethyl acrylate)- was purified using neutral Aluminum Oxide column to remove the inhibitor then dried in an oven at 55 °C [27].

TABLE 1. Physical and chemical properties of formation water.

Chemical properties	Unit (ppm)	Physical properties	
Sodium and potassium	2205	pH	6.88
Magnesium	46	Salinity as NaCl	7449
Barium	3.74	Total alkalinity	310
Strontium	6.50	Total hardness	842
Chlorides	4537	Temporary hardness	310
Sulphates	1750	Permanent hardness	532
Bicarbonates	378		
T.D.S.	11000		

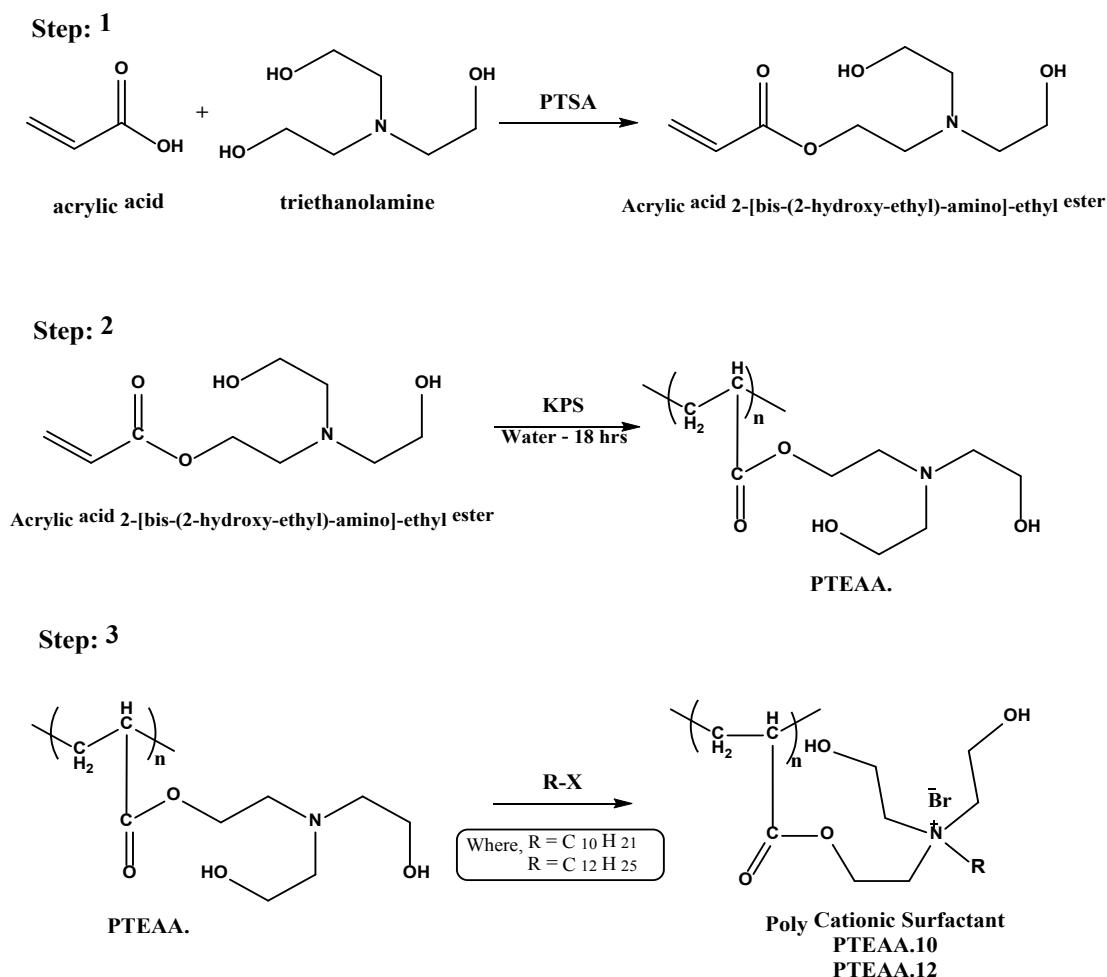
Homopolymerization of (2-(bis(2-hydroxy) amino) ethyl acrylate)

The polymerization reaction was achieved in small test tubes equipped with magnetic stirrers. About 2.21 g of the freshly prepared monomer was introduced into the tube with an appropriate amount of distilled water. Initiator KPS (potassium persulphate) was added. The tubes were deoxygenated by flushing them with Nitrogen gas for twenty min, sealed with aluminum foil and then placed in a water bath at 70 °C for 18 h with vigorous stirring. Then, the reaction was terminated by immersing the test tubes in an ice bath at 0 °C for 1 h with continuous stirring. The result was a slightly viscous liquid that was decanted into methanol at a ratio of 1:10 v/v with agitation and was allowed to stand at room

temperature overnight. Then after, the solvent was decanted and the polymer was obtained, which named PTEAA [28].

Quaternization of the prepared polymeric surfactants

Quaternization reactions of 0.1 mol of the prepared polymer (PTEAA) with 0.12 mol of different alkyl bromides (1-bromodecane and 1-bromododecane) were carried out in ethanol at 70 °C for 48 h to produce two polymeric cationic surfactants (PTEAA.10 and PTEAA.12). The reaction mixture was permitted to cool down. The produced cationic surfactant was further refined by diethyl ether then recrystallized from ethanol. The steps of the reaction are illustrated in Scheme 1.



Scheme 1. Synthetic procedure of the polymeric cationic surfactants (PTEAA.10 and PTEAA.12).

Evaluation of the polycationic surfactants (PTEAA.10 and PTEAA.12) as corrosion inhibitors

Preparation of inhibitor solutions

The PTEAA.10 and PTEAA.12 inhibitors were added to the untreated tested formation water at various concentrations of 50, 100, 150, 200, and 250 ppm by weight. All the inhibitors are soluble in bidistilled water.

Weight loss

X65 carbon steel was cut into rectangular shapes of 40.14 cm² area for each. Before each test, specimens were mechanically polished in a sequential manner with different SiC emery paper grades (320, 107 400, 600, 1200 and 2000 grit). Then, the polished specimens were washed with distilled water, rinsed with ethanol and acetone and finally dried between two filter papers and weighed. The weight loss test method was performed according to ASTM D2688) by immersing the polished specimens in formation water containing cationic surfactants for 90 days [7,29].

The inhibition efficiency (I%) was calculated from the following equation [30]:

$$I\% = \frac{W - W_0}{W} \cdot 100 \quad (1)$$

Where W and W_0 are the weight loss per unit area in the absence and presence of inhibitor, respectively. Through studying the effect of inhibition efficiency, the rate of corrosion (C_{rate}) was calculated by the following equation [29]:

$$C_{rate} = \frac{\Delta W \cdot 3.45 \cdot 10^6}{A \cdot t \cdot D} \quad (2)$$

Where, ΔW is the mass loss in gram, A , is the area in cm², t , is the immersion time in hours, D , is density of carbon steel (7.87 gm.cm⁻³).

Electrochemical tests

The electrochemical experiments were performed using three electrodes-system: saturated calomel electrode and platinum electrode as Reference and counter electrodes respectively and X65 carbon steel as the working electrode in the double jacket cell (100 ml) using a Voltalab 40 Potentiostat PGZ 301 combined with software (Voltmaster 4).

The working electrode (carbon steel) was cut and shaped into a cylindrical form of 1 cm² cross-section area. Then embedded in *Egypt.J.Chem.* **63**, No. 3 (2020)

polytetrafluoroethylene (PTFE)-based epoxy resin. The exposed electrode area to the corrosive solution was 1 cm². The working electrode was abraded with a series of emery papers, degreased in ethanol, washed with distilled water and finally dried. The polarization curves were measured at a scan rate of 2 mVs⁻¹ and all the measurements were carried out at 298.15 K. Current-potential curves were recorded by changing the electrode potential automatically with a scan rate 2 mV s⁻¹ from a low potential of -800 to -300 mV (SCE)[31].

Electrochemical impedance (EIS) measurements were performed within a frequency range of 100 kHz to 50 mHz with a 4 mV sine wave as the excitation signal at open circuit potential. Electrochemical parameters obtained from EIS and Tafel were fitted using Zimpview software [32, 33].

Surface characterization

Surface analysis of carbon steel was performed using SEM model QUANTA FEG 250 (Field Emission Gun); High 138 resolution (106X) attached with EDAX unite (Energy Dispersive X-ray Analyzer). Morphological changes on the surface of X65 carbon steel were investigated before and after immersion in formation water containing 250 ppm PTEAA.12 for 16 days[34].

Result and Discussion

Spectroscopic analysis of the PTEAA.12 compound

FT-IR of the prepared compounds Triethanolamine acrylate monoester, Homopolymer, and Quaternized Homopolymer abbreviated (TEAA, PTEAA, and PTEAA.12) respectively were shown in (Fig. 1a, b and c) respectively. From Fig. 1a, it can be observed that, sharp peak at 1732 cm⁻¹ due to the carbonyl group of the ester compound; peak at 1660 cm⁻¹ due to the double bond of acrylate and broad peak at 3386 cm⁻¹ for hydroxyl group of triethanolamine. As shown in Fig. 1b, the disappearance of C=C peak and shifting in ester to 1734 cm⁻¹ due to Homopolymerization of the triethanolamine acrylate. FT-IR of the cationic surfactant (PTEAA.12) shown in Fig 1c, showed a sharp peak at (1072 cm⁻¹) for (N⁺) together with multi-broad peaks at (2050-3200 cm⁻¹), and two strong absorption peaks at 2895 cm⁻¹ and 2929 cm⁻¹ due to stretching and bending vibrations of (CH₃) and (CH₂) of the long alkyl chain due to quaternization reaction.

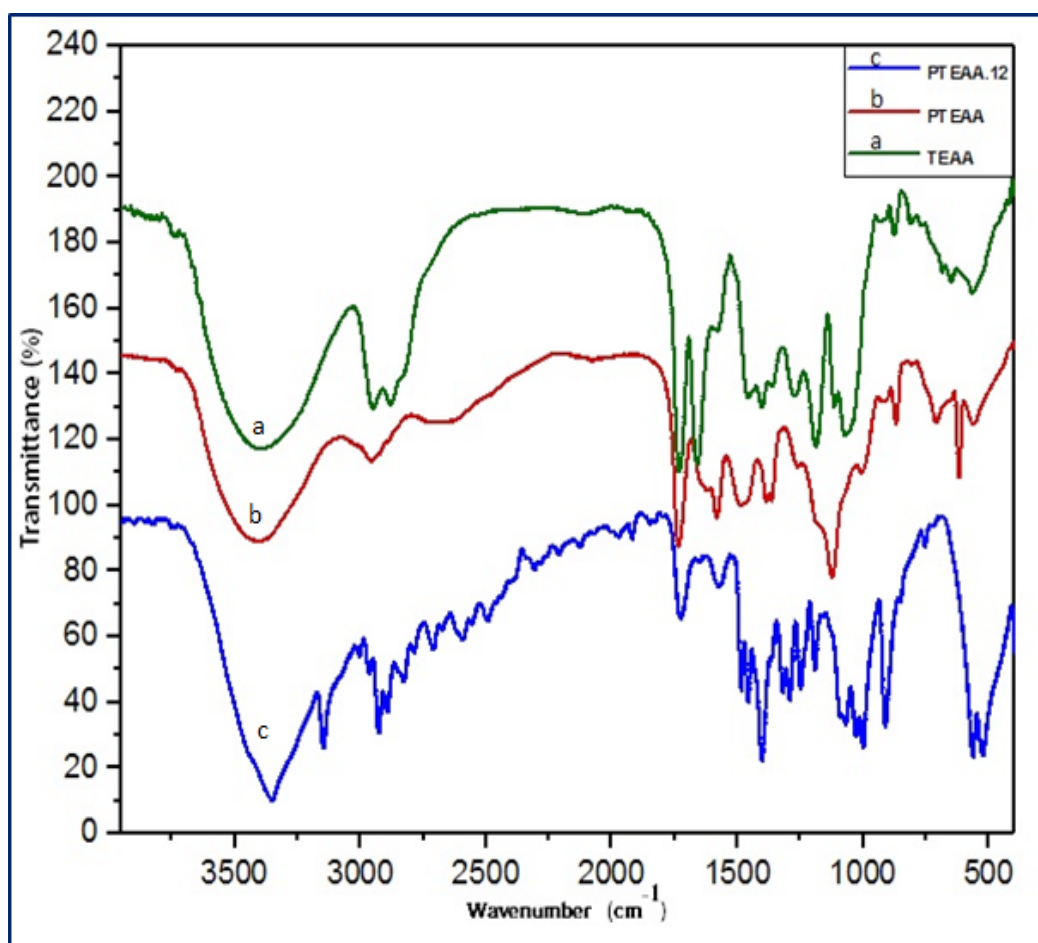


Fig. 1. FT-IR spectrum of (a) TEAA. (b) PTEAA. and (c) PTEAA.12.

The ^1H NMR and ^{13}C NMR spectra of PTEAA.12 in (DMSO) as a representative sample for the synthesized polycationic surfactants are shown in Fig 2a and 2b, respectively.

Figure 2a showed different ^1H NMR signals at the following chemical shifts $\delta = 0.98$ ppm for $(\text{N}^+\text{CH}_2(\text{CH}_2)_n\text{CH}_3)$; $\delta = 1.2$ ppm for $(\text{N}^+\text{CH}_2(\text{CH}_2)_n\text{CH}_3)$; $\delta = 1.4$ ppm for $(\text{OCO}-\text{CHCH}_2-)$; $\delta = 2.1$ ppm for (OCOCH_2-) ; $\delta = 3.1$ ppm for $(\text{N}^+\text{CH}_2(\text{CH}_2)_n\text{CH}_3)$; $\delta = 3.4$ ppm for $(\text{N}^+\text{CH}_2\text{CH}_2\text{OH})$; $\delta = 3.9$ ppm for $(\text{N}^+\text{CH}_2\text{CH}_2\text{OH})$; $\delta = 3.9$ ppm for $(\text{N}^+\text{CH}_2\text{CH}_2\text{OCO})$; and $\delta = 4.11$ ppm for $(\text{N}^+\text{CH}_2\text{CH}_2\text{OCO})$.

^{13}C NMR (DMSO) spectrum of PTEAA.12 represented in Fig. 2.b, illustrated different signals at $\delta = 14.1$ ppm for $(\text{N}^+\text{CH}_2\text{CH}_2(\text{CH}_2)_9\text{CH}_2\text{CH}_3)$; $\delta = 22$ ppm for $(\text{N}^+\text{CH}_2\text{CH}_2(\text{CH}_2)_9\text{CH}_2\text{CH}_3)$; $\delta = 24.2$ ppm for $(\text{N}^+\text{CH}_2\text{CH}_2(\text{CH}_2)_9\text{CH}_2\text{CH}_3)$; $\delta = 28.2$ ppm for $(\text{N}^+\text{CH}_2\text{CH}_2(\text{CH}_2)_9\text{CH}_2\text{CH}_3)$; $\delta = 29.5$ ppm for $(\text{N}^+\text{CH}_2\text{CH}_2(\text{CH}_2)_9\text{CH}_2\text{CH}_3)$;

$\delta = 31.8$ ppm for $(\text{N}^+\text{CH}_2\text{CH}_2(\text{CH}_2)_9\text{CH}_2\text{CH}_3)$; $\delta = 56$ ppm for $(\text{N}^+\text{CH}_2\text{CH}_2\text{OH})$; $\delta = 60,62$ ppm for $(\text{N}^+\text{CH}_2\text{CH}_2\text{OCO})$ respectively; $\delta = 64$ ppm for $(\text{N}^+\text{CH}_2\text{CH}_2\text{OH})$ and $\delta = 173.9$ ppm for $(\text{N}^+\text{CH}_2\text{CH}_2\text{OCO})$.

Corrosion investigation

Weight loss

The weight loss technique was carried out to study the effect of inhibitor concentration on the inhibition performance for carbon steel (X65) in formation water at 298 K for 90 days. This behavior could be attributed to the increase of the surface area covered by the adsorbed molecules of polycationic surfactant as well as with the rise in its concentration. The inhibitory action attributes to active poly sites which are electron donors (heteroatoms); simply many active sites. So the inhibition effect increases as the concentration increases; reaches the optimum values. i.e., 92.8% and 84.7% for PTEAA.12 and PTEAA.10, respectively at 250 ppm.

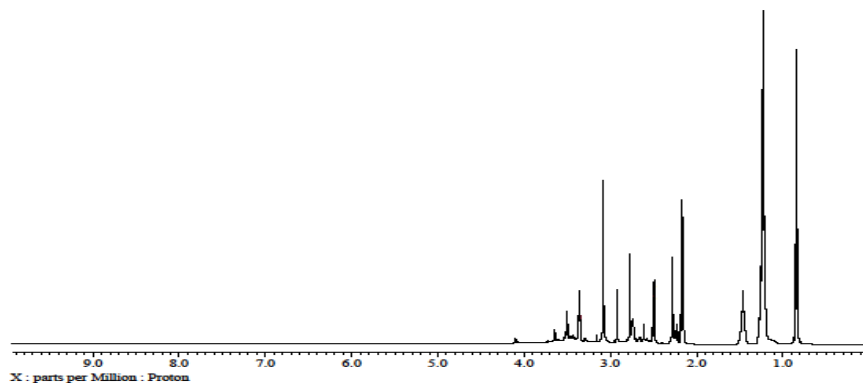


Fig. 2a. $^1\text{H-NMR}$ (DMSO) spectrum of PTEAA.12 polycationic surfactant.

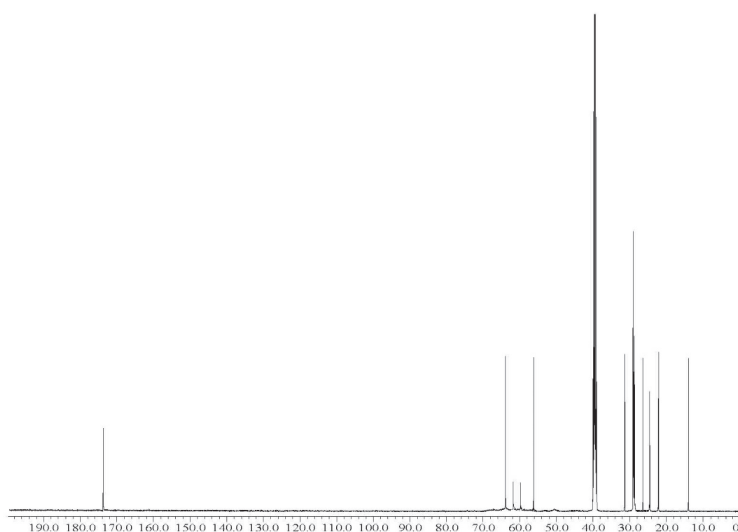


Fig. 2b. $^{13}\text{C-NMR}$ (DMSO) spectrum of PTEAA.12 polycationic surfactant.

The surface coverage (θ) was calculated by the following equation [35]:

$$\theta = \frac{W - W_0}{W_0} \quad (3)$$

Where W and W_0 are the weight of tested carbon steel before and after immersion in the tested formation water. θ and $I\%$ values are calculated using equations (1 & 3) and summarized in Table 2. It was found that, the inhibition performance of the two inhibitors increases with increasing their

concentrations. It can also be observed that the PTEAA.12 inhibits the steel surface more than PTEAA.10, and this may be due to increasing the carbon chain length, which enhanced the adsorption process [33, 36]. The C_{rate} in the function of concentration and molecular weight of the prepared inhibitors. So, from the tabulated data Table 2, the C_{rate} decrease gradually with increasing the concentration till reach 0.15 mpy and 0.32 mpy for PTEAA.12 and PTEAA.10, respectively at 250.

TABLE 2. Data obtained from weight loss measurements of carbon steel in formation water in the absence and presence of various concentrations of PTEAA.10 and PTEAA.12 at 298 K for 90 days.

Inhibitor	Conc. (ppm)	Θ	I %	CR(mpy)
PTEAA.10	50	0.53	53.81	0.97
	100	0.75	75.47	0.52
	150	0.78	78.78	0.44
	200	0.80	80.64	0.41
	250	0.84	84.67	0.32
PTEAA.12	50	0.57	57.93	0.89
	100	0.78	78.97	0.44
	150	0.83	83.31	0.35
	200	0.86	86.29	0.29
	250	0.92	92.82	0.15

Electrochemical impedance spectroscopy measurements (EIS)

EIS is a unique technique to study the electrochemical resistance parameters for the corrosion phenomenon of carbon steel. Fig. 3a and 3b represent the Nyquist and Bode plots of X65 immersed in formation water with and without different doses of the polycationic surfactants PTEAA.10 and PTEAA.12, respectively. The close inspection of Nyquist diagram reveals the presence of two badly separated depressed capacitive loops with two time-constant. This depression is related to frequency dispersion phenomenon [37, 38].

The shape of Nyquist diagram still not changed after the addition of the inhibitor. This means that the corrosion reaction mechanism of X65 doesn't change [39]. The diameter of the depressed semicircle is function in concentration and hydrophobicity, i.e. the diameter increased as Concentration and carbon chain length increase, respectively. Fig 3c. represents the comparison of bode plots of the highest concentrations (250 ppm) for PTEAA.10 and PTEAA.12 referenced to the blank [40].

Modulus $|Z|$ increase with the presence of the inhibitors and further increase with hydrophobicity. Equivalent circuit in Fig. 4. is used to analyze the EIS experimental data for polymeric cationic surfactants (PTEAA.10 and PTEAA.12) where R_s is solution resistance, R_{ct} is charge transfer resistance, R_f is film resistance and Q_{ct} , and Q_f are the double layer capacitance of X65 and the formed film, respectively.

The fitted data are recorded in Table 3 and noticed that the values of R_{ct} and R_f increased while the values of Q_f and Q_{ct} decreased. The Q_f and C_{dl} were decreased as a result of increasing the thickness of electrical double layer due to the increase in the inhibitors concentrations. This can be ascribed to the change of water molecules in the vicinity of carbon steel surface by the adsorbed inhibitor molecules. That produces an adherent protective layer at the carbon steel surface which decreases the local dielectric constant of the carbon steel/solution interface [41].

These observations may be due to the incorporation of the inhibitor molecules with the corrosion film increases corrosion resistance. R_{ct} value increased significantly with the addition of PTEAA.10 and PTEAA.12.

The inhibition efficiency is calculated from equation [42]:

$$E_i\% = \left(\frac{R_{ct(inh)} - R_{ct(0)}}{R_{ct(inh)}} \right) \times 100 \quad (4)$$

Where $R_{ct(0)}$ and $R_{ct(inh)}$ are charge transfer resistance without and with of inhibitors, respectively.

The inhibition efficiency increased with increasing the concentration and reached 86.98% at optimum concentration of PTEAA.12. The inhibition efficiencies of the used inhibitor PTEAA.12 higher than PTEAA.10 which is in a good agreement with the results obtained from Tafel polarization and weight loss evaluation [43, 44].

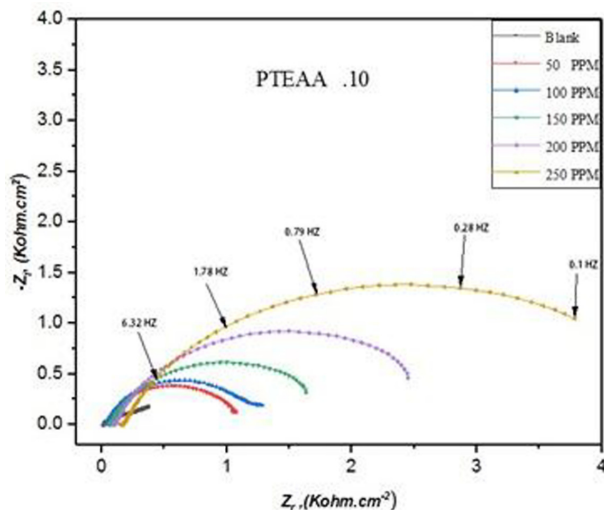


Fig. 3a. Nyquist plot of X65 carbon steel working electrode in absence and presence of PTEAA.10 inhibitor at different concentrations.

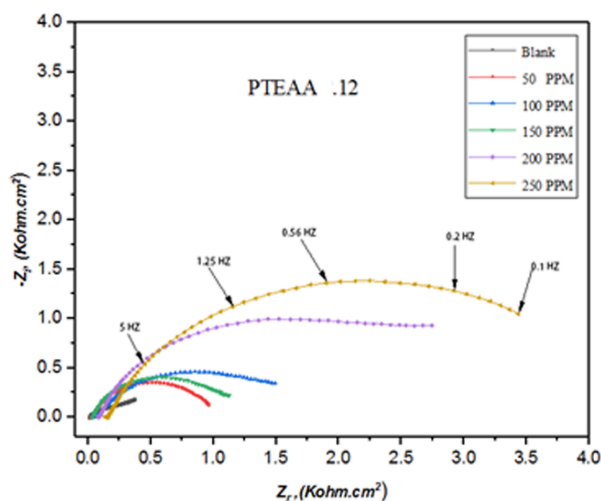


Fig. 3b. Nyquist plot of X65 carbon steel working electrode in absence and presence of PTEAA.12 inhibitor at different concentrations.

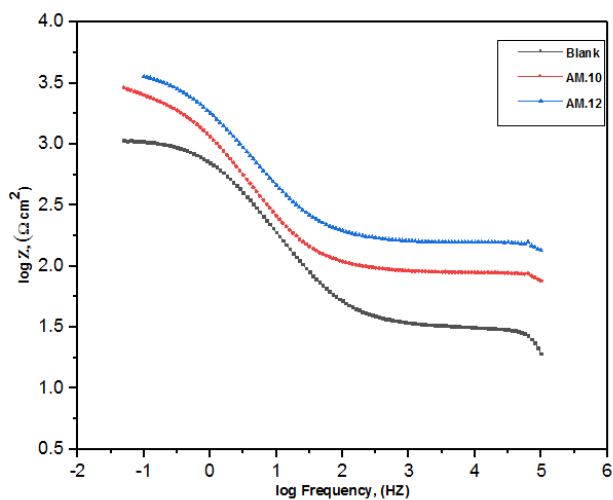


Fig. 3c. Bode plot for X65 in formation water without and with 250 ppm concentration of the prepared poly cationic surfactants PTEAA.10 and PTEAA.12 at 298 K.

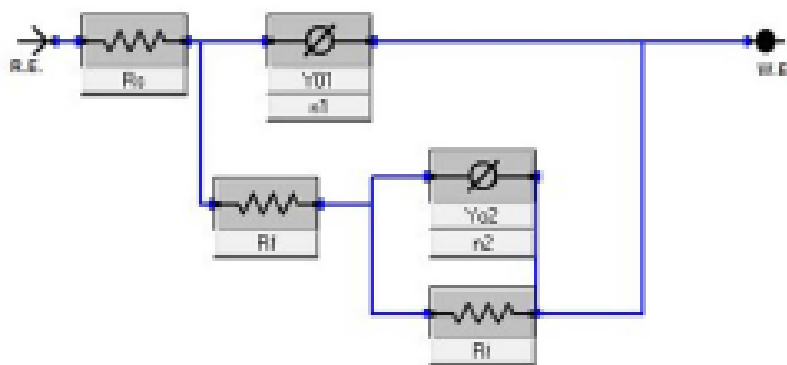


Fig. 4. Equivalent electrical circuit diagram.

TABLE 3. EIS parameters for X65 engrossed in formation water in absence and presence of different concentrations of inhibitors.

Inhibitor	Conc. (ppm)	R_s ($\Omega \text{ cm}^2$)	C_p ($\mu\text{F} \cdot \text{Cm}^2$)	n_1	R_p ($\Omega \text{ cm}^2$)	Cdl , ($\mu\text{F}/\text{Cm}^2$)	n_2	R_{ct} , ($\Omega \text{ cm}^2$)	$\eta\%$
-	Blank	0.03	14.9	0.651	13.21	77.5	0.731	570	-
	50	0.052	12.8	0.662	14.51	70.01	0.752	1102.5	39.23
	100	0.0762	11.1	0.668	16.92	62.5	0.759	1501.5	55.38
PTEAA.10	150	0.0893	10.2	0.682	19.51	45.2	0.761	2362.5	71.64
	200	0.116	8.9	0.701	20.5	41.1	0.801	3202.5	79.08
	250	0.162	8.09	0.702	29.5	30.1	0.811	4150	83.86
	50	0.06	10.5	0.672	16.2	68.25	0.756	1281	47.70
	100	0.057	9.08	0.692	18.5	60.10	0.763	2205	69.61
PTEAA.12	150	0.041	8.12	0.712	20.1	41.21	0.795	3129	78.59
	200	0.080	6.45	0.725	28.4	39.8	0.812	4311	84.46
	250	0.159	5.81	0.742	35.6	28.1	0.815	5145	86.98

Potentiodynamic (Tafel) polarization measurements

Figure 5a and 5b, show the cathodic and anodic polarization curves of carbon steel immersed in formation water in the absence and presence of different concentrations of PTEAA.10 and PTEAA.12, respectively.

Electrochemical parameters such as the corrosion potential (E_{corr}), corrosion current density (I_{corr}), and cathodic and anodic Tafel slopes (β_c and β_a) were calculated and listed in Table 4. The inhibition efficiency ($IE\%$) values were evaluated from the measured I_{corr} values using the following equation [45, 46]:

$$IE\% = \left[\left(\frac{I_{corr} - I_{corr(inh)}}{I_{corr}} \right) \right] * 100 \quad (5)$$

Where, I_{corr} and $I_{corr(inh)}$ are the corrosion current values without and with the addition of

various concentrations of inhibitor. From Fig. 5b, it is clear that both the anodic metal dissolution and cathodic reduction reactions were inhibited when compound PTEAA.12 was added to the formation water and this inhibition was more pronounced with increasing inhibitor concentration. The Tafel lines were shifted from more negative to more positive potentials with respect to the blank curve by increasing the concentration of the inhibitor. The results tabulated in Table 4, show that an increase in the inhibitor concentration leads to a decrease in the corrosion current density (I_{corr}), the shapes of tafel curves were not changed by the addition of the inhibitor so the X65 corr. Mechanism was not changed.

The shifting in E_{corr} value was in range (-66mV) i.e less than ($\pm 85\text{mV}$) so, the prepared PTEAA.10 and PTEAA.12 could be act as mixed inhibitors [47].

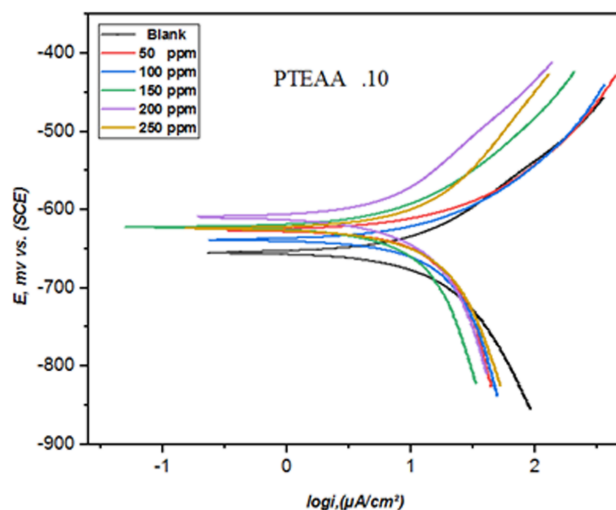


Fig. 5a. Potentiodynamic polarization curves (E - $\log I$ relationship) of carbon steel in formation water in the absence and presence of different concentrations of PTEAA.10.

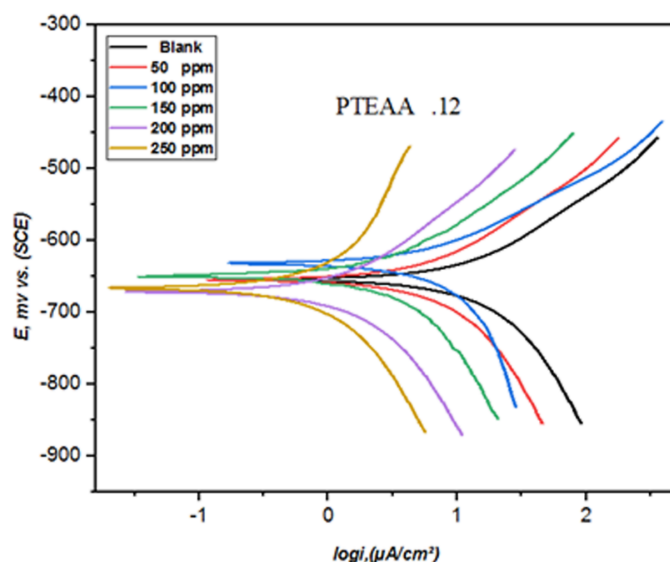


Fig. 5b. Potentiodynamic polarization curves (E - $\log I$ relationship) of carbon steel in formation water in the absence and presence of different concentrations of PTEAA.12.

TABLE 4. Data obtained from potentiodynamic polarization measurements of X65 in formation water solution in the absence and presence of various concentrations of compounds PTEAA.10 and PTEAA.12 at 298 K.

Inhibitors	Conc. Ppm	$-E_{\text{corr}}$, mv	I_{corr} , $\mu\text{A}/\text{cm}^2$	Θ	IE_T %
PTEAA.10	Blank	654.4	22.7688
	50	625.9	12.8128	0.437	43.73
	100	638	7.7073	0.661	66.15
	150	621.8	5.3916	0.763	76.32
	200	609.2	4.5718	0.799	79.92
	250	623.9	2.9643	0.869	86.98
PTEAA.12	50	654.4	11.3824	0.500088	50.01
	100	631.8	5.2456	0.769615	76.96
	150	648.7	4.3543	0.80876	80.88
	200	671	3.872	0.829943	82.99
	250	666.1	2.254	0.901005	90.10

The obtained results indicate that the percentage inhibition efficiency (IE%) of compound PTEAA.12 is greater than that of compound PTEAA.10 by 90.1% and 86.98% respectively. The order of inhibition efficiency was PTEAA.12 > PTEAA.10 and this in agreement with the previous techniques (WL & EIS).

Adsorption isotherm calculations

Type of the corrosive environment, the chemical structure of an organic inhibitor, the distribution of charge in the molecule and the nature properties of the metal surface, etc are the major factors that affect the adsorption of inhibitor and inhibition process on the metal surface [48]. Adsorption process has been done by applying different adsorption isotherm modules such as Langmuir, Frumkin, Temkin, Freundlich and Flory–Huggins adsorption isotherms as listed in the supplementary data that were shown in Fig. S (1, 2, 3, and 4) respectively [49-51]. Moreover, the best fitted module was Langmuir adsorption isotherm due to highly R^2 and unity of slope that are shown in as shown in Fig. 6a and Fig. 6b. The Langmuir isotherm is described according to the following equation [52]:

$$\frac{C_{inh}}{\theta} = C_{inh} + \frac{1}{K_{ads}} \quad (6)$$

Where, K_{ads} is the equilibrium constant for the adsorption– desorption process, C_{inh} is molar concentration of inhibitor in the bulk solution and θ is the degree of surface coverage. From K_{ads} values ΔG_{ads}° can be calculated using the following equations [53, 54]:

$$\Delta G_{ads}^{\circ} = -RT \ln[(10)^6 * K_{ads}] \quad (7)$$

Where T is the absolute temperature, R is the gas constant, and 10^6 is the concentration of water in ppm. The high K_{ads} value reflects the high adsorption ability of both Polymeric cationic (PTEAA.10 and PTEAA.12) surfactants were 150 and $212 \times 10^4 \text{ kJ mol}^{-1}$ as shown in Table 5. This suggested that the adsorption phenomenon took place spontaneously via physical adsorption.

Surface examinations by SEM/EDX

In order to confirm the formation of a protective film of the inhibitors at the electrode surface, SEM/EDX examinations of the metal surface were performed. The morphologies and EDX analysis of the C steel samples exposed for

14 days in the uninhibited and inhibited formation water samples at 298.15 K are shown in Fig. 8 (a, b, c).

Figure 7a shows SEM and EDX analysis for polished X-65 carbon steel surface. Fig. 7b shows the surface of carbon steel (blank sample) that was immersed in formation water without any cationic surfactant, where the corrosion products Fe (Cl, O) and mineral deposited formation make the surface is thoroughly damaged. The coupled EDX spectrum shows characteristic signals for Fe and Ca. this damage may be from the severe attack of the metal surface by anions constituents in the test solution and formation of scale products. the Fe peak intensity was low indicating the formation of a thick porous layer from corrosion and scale products covered the electrode surface [43]. The metal sample immersed in 250 ppm PTEAA.12 inhibited formation water, on the contrary, displayed tangibly improved surface, (Fig. 7c) compared to the blank sample. Moreover, EDX spectra show a strong peaks for Ca, Cl and O signals contribution. The Fe peak intensity obviously increased compared to the blank solution indicating the absence of thick corrosion and scale layer. These observations confirm the anticorrosion behaviour of the prepared surfactants for X65 steel in the formation water which is well agree with other electro chemical results [42, 55].

Conclusion

1. Two polymeric cationic surfactants were prepared based on Triethanolamine acrylate.
2. The chemical structure of the prepared poly cationic surfactants was confirmed by FT-IR, ¹H NMR and GPC techniques.
3. The prepared compounds were evaluated as corrosion inhibitors for Carbon Steel in formation water.
4. Three techniques were used in the corrosion inhibition evaluation.
5. The inhibition performance for the prepared poly cationic surfactants increases by increasing the concentration as well as the alkyl chain length.
6. The prepared inhibitors act as mixed types corrosion inhibitors and the adsorption obeys the Langmuir adsorption isotherm.
7. Results obtained from SEM and EDX techniques were in agreement with the corrosion inhibition evaluation techniques.

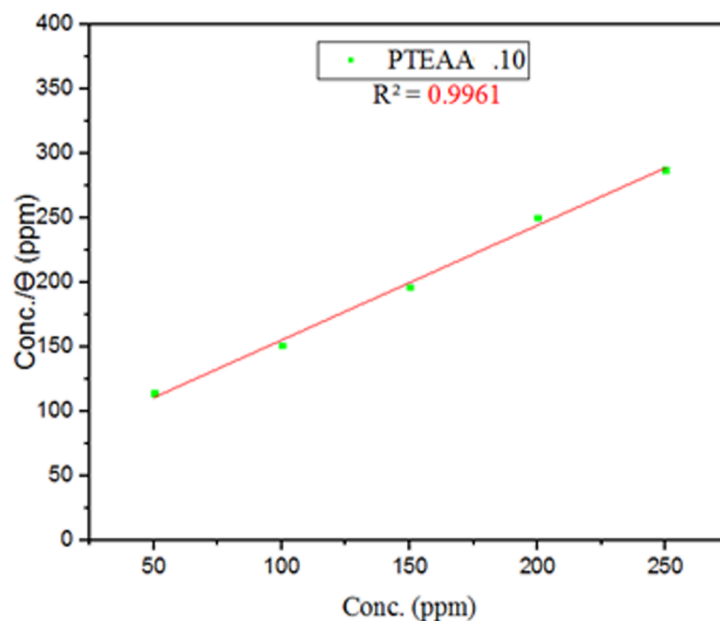


Fig. 6a. Langmuir adsorption isotherm curve (Conc./ Θ vs. Conc.) obtained from polarization data for synthesized inhibitor (PTEAA.10).

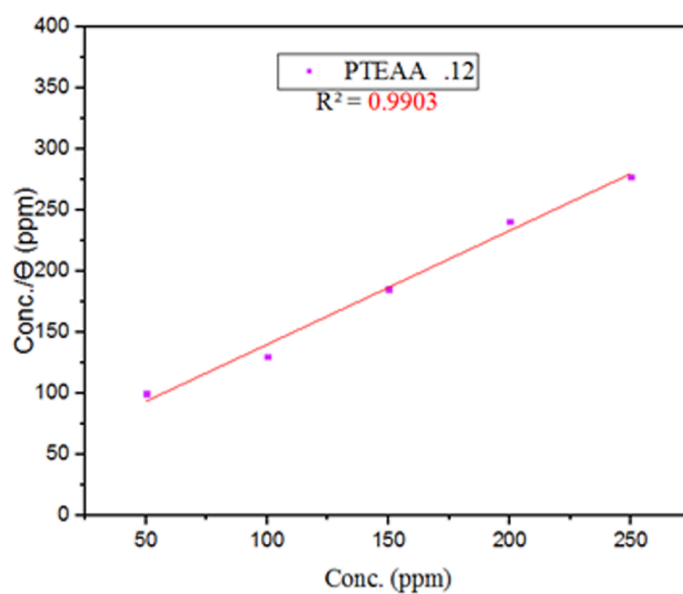


Fig. 6b. Langmuir adsorption isotherm curve (Conc./ Θ vs. Conc.) obtained from polarization data for synthesized inhibitor (PTEAA.12).

TABLE 5. Langmuir adsorption isotherm parameters for the synthesized inhibitors.

Inhibitor	Slope	Regression coefficient (R ²)	K _{ads} (10 ⁴)	ΔG_{ads} (kJ)
PTEAA.10	0.8904	0.9961	150.65	-23.8389
PTEAA.12	0.9320	0.9903	212.94	-24.6964

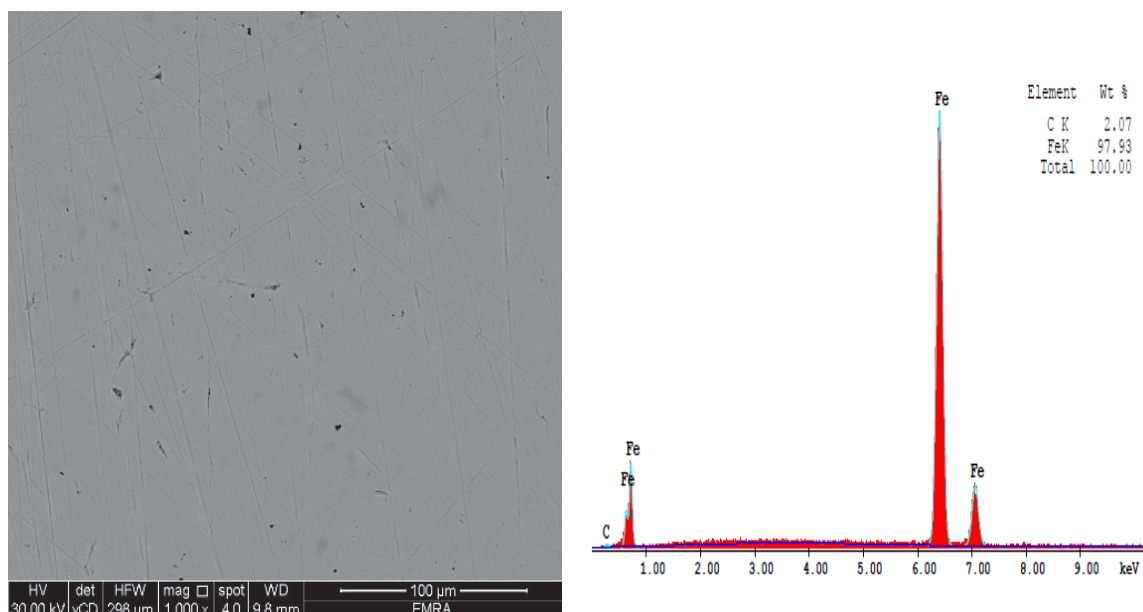


Fig. 7a. SEM and EDX analysis for polished X-65 carbon steel surface.

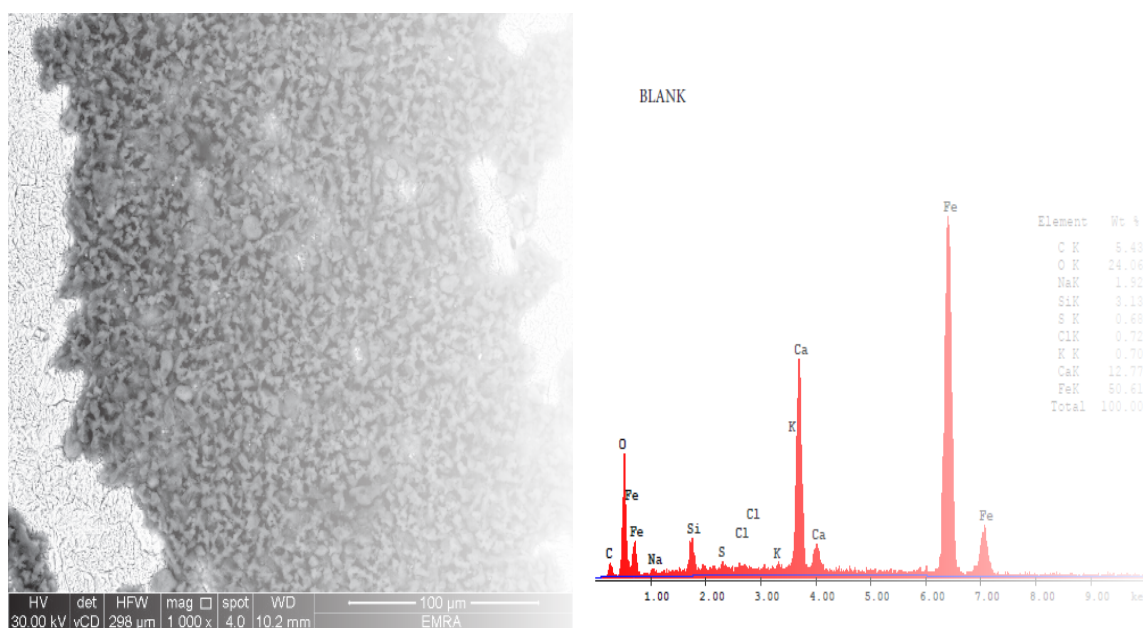


Fig. 7b. SEM and EDX analysis for X-65 carbon steel surface after immersion in test solution (formation water) in absence of polycationic surfactants for 14 days.

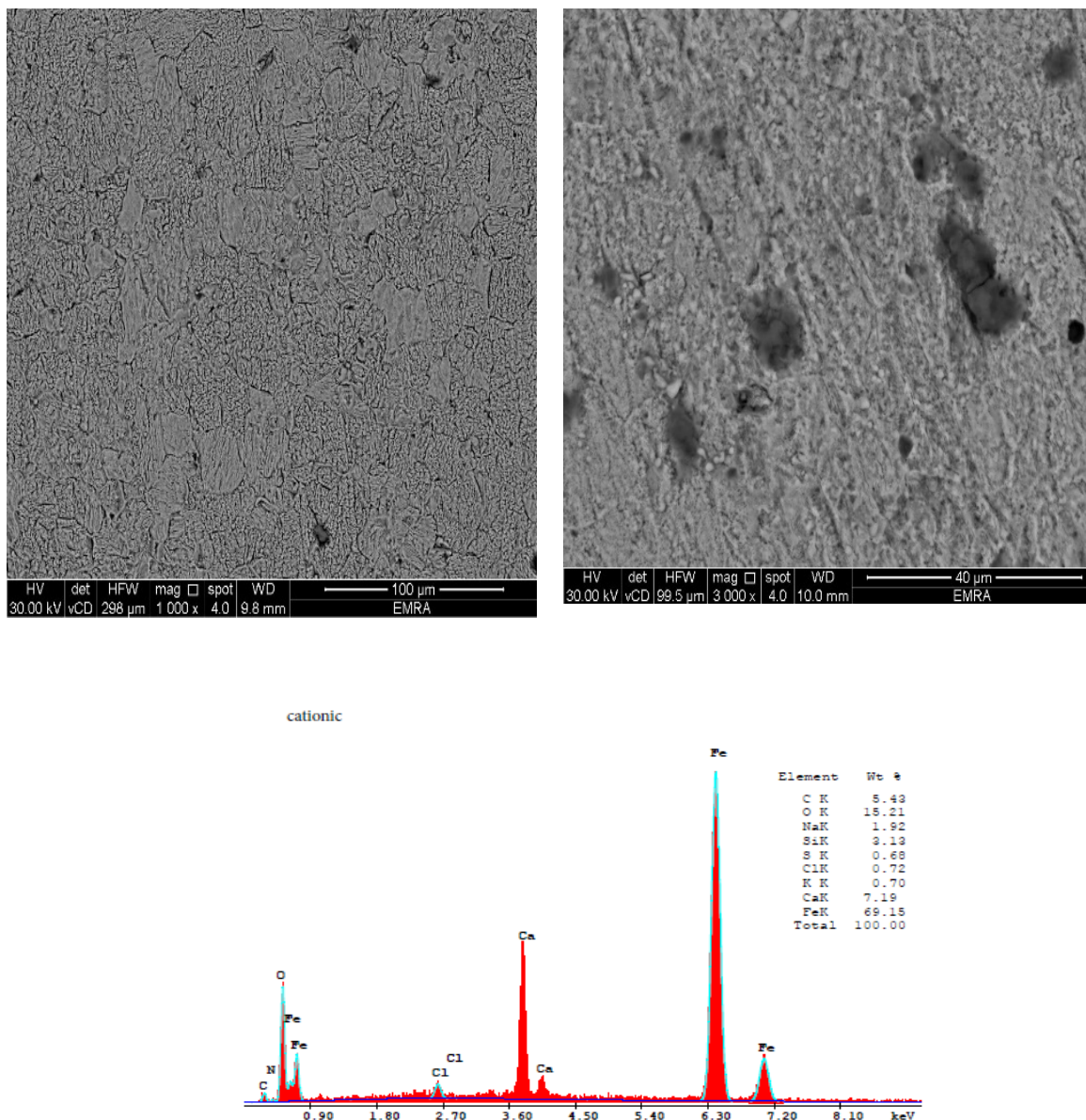


Fig. 7c. SEM micrographs at two different magnifications, and EDX analysis for X-65 carbon steel surface after immersion in test solution containing 250 ppm of inhibitor (PTEAA.12) at 298 K for 14 days.

References

- Bauer S., Schmuki P., Von Der Mark K. and Park J., Engineering biocompatible implant surfaces: Part I: Materials and surfaces. *Progress in Materials Science*, **58** (3), 261-326 (2013).
- Jenck J.F., Agterberg F. and Droescher M.J., Products and processes for a sustainable chemical industry: a review of achievements and prospects. *Green Chemistry*, **6** (11), 544-556 (2004).
- Kritzer P., Boukis N. and Dinjus E., Factors controlling corrosion in high-temperature aqueous solutions: a contribution to the dissociation and solubility data influencing corrosion processes. *The Journal of supercritical fluids*, **15** (3), 205-227 (1999).
- Jacob K.S. and Parameswaran G., Corrosion inhibition of mild steel in hydrochloric acid solution by Schiff base furoin thiosemicarbazone. *Corrosion Science*, **52** (1), 224-228 (2010).
- Fakhru'l-Razi A., Pendashteh A., Abdullah L.C., Biak D.R.A., Madaeni S.S. and Abidin Z.Z., Review of technologies for oil and gas produced water treatment. *Journal of hazardous materials*, **170** (2-3), 530-551 (2009).

6. Ismail N., Megahed H., Ali A. and Eletre M.A., Application of Theophylline Anhydrous as Inhibitor of Acid Corrosion of Aluminum. *Egyptian Journal of Chemistry*, **60** (1), 95-107(2017).
7. Alsabagh A., Migahed M. and Awad H.S., Reactivity of polyester aliphatic amine surfactants as corrosion inhibitors for carbon steel in formation water (deep well water). *Corrosion Science*, **48** (4), 813-828 (2006).
8. Abdelaal M.M., Mohamed S., Barakat Y.F., Derbala H.A.Y., Hassan H.H. and Al Zoubi W., N-Aminophthalimide as a Synthone for Heterocyclic Schiff bases: Efficient Utilization as Corrosion Inhibitors of Mild Steel in 0.5 mol.L⁻¹ H₂SO₄ Solution. *Egyptian Journal of Chemistry*, **61**(3), 539-558 (2018).
9. Osman M.M. and Shalaby M.N., Some ethoxylated fatty acids as corrosion inhibitors for low carbon steel in formation water. *Materials Chemistry and Physics*, **77** (1), 261-269(2003).
10. Deyab M.A., Inhibition activity of Seaweed extract for mild carbon steel corrosion in saline formation water. *Desalination*, **384**, 60-67(2016).
11. Alsabagh A.M., Migahed M.A. and Awad H.S., Reactivity of polyester aliphatic amine surfactants as corrosion inhibitors for carbon steel in formation water (deep well water). *Corrosion Science*, **48** (4), 813-828 (2006).
12. Migahed M.A., Farag A.A., Elsaed S.M., Kamal R., Mostfa M. and El-Bary H.A., Synthesis of a new family of Schiff base nonionic surfactants and evaluation of their corrosion inhibition effect on X-65 type tubing steel in deep oil wells formation water. *Materials Chemistry and Physics*, **125** (1), 125-135 (2011).
13. Donahue F.M. and Nobe K., Theory of organic corrosion inhibitors adsorption and linear free energy relationships. *Journal of the Electrochemical Society*, **112** (9), 886-891(1965).
14. Jevremović I., Singer M., Nešić S. and Mišković-Stanković V., Inhibition properties of self-assembled corrosion inhibitor talloil diethylenetriamine imidazoline for mild steel corrosion in chloride solution saturated with carbon dioxide. *Corrosion Science*, **77**, 265-272 (2013).
15. Assem Y., Abu-Zeid R., Ali K. and Kamel S., Synthesis of Acrylate-Modified Cellulose via Raft Polymerization and Its Application as Efficient Metal Ions Adsorbent. *Egyptian Journal of Chemistry*, **62** (1), 85-96 (2019).
16. Almzarzie K., Falah A., Massri A. and Kellawi H., Electrochemical Impedance Spectroscopy (EIS) and Study of Iron Corrosion Inhibition by Turmeric Roots Extract (TRE) in Hydrochloric Acid Solution. *Egyptian Journal of Chemistry*, **62** (3), 501-512(2019).
17. Tharanathan R., Biodegradable films and composite coatings: past, present and future. *Trends in food science & technology*, **14** (3), 71-78(2003).
18. Zhang G., Wu H.B., Hoster H.E. and Lou X.W.D., Strongly coupled carbon nanofiber-metal oxide coaxial nanocables with enhanced lithium storage properties. *Energy & Environmental Science*, **7** (1), 302-305 (2014).
19. Ameer M.A., Abdel Hamid Z., Shehata M., Hassan B.M. and Fekry A.M., The Impact of Cationic Surfactants on The Electrodeposition of Nickel/ Graphene Nano-Sheet Composite Coatings on Brass. *Egyptian Journal of Chemistry*, **62** (2), 201-214 (2019).
20. El Achouri M., Infante M.R., Izquierdo F., Kertit S., Gouytaya H. and Nciri B., Synthesis of some cationic gemini surfactants and their inhibitive effect on iron corrosion in hydrochloric acid medium. *Corrosion Science*, **43** (1), 19-35(2001).
21. El Achouri M., Kertit S., Gouytaya H., Nciri B., Bensouda Y., Perez L., Infante M. and Elkacemi K., Corrosion inhibition of iron in 1 M HCl by some gemini surfactants in the series of alkanediyl- α , ω -bis-(dimethyl tetradecyl ammonium bromide). *Progress in Organic Coatings*, **43** (4), 267-273 (2001).
22. Al-Sabbagh A., Osman M., Omar A. and El-Gamal I., Organic corrosion inhibitors for steel pipelines in oilfields. *Anti-corrosion methods and materials*, **43** (6), 11-16 (1996).
23. El Wanees S.A., Alahmadi M.I., Alsharif M.A. and Atef Y., Mitigation of Hydrogen Evolution during Zinc Corrosion in Aqueous Acidic Media Using 5-Amino-4-imidazolecarboxamide. *Egyptian Journal of Chemistry*, **62** (5), 10-11 (2019).
24. Rosen M.J. and Kunjappu J.T., Surfactants and interfacial phenomena, John Wiley & Sons (2012).
25. Salem a.m. and Fouda A., Calicotome Extract as a Friendly Corrosion Inhibitor for Carbon Steel in Polluted NaCl Solution: Chemical and Electrochemical Studies. *Egyptian Journal of Chemistry*, DOI 10.21608/ejchem.2019.7656.1649 (2019).

26. Migahed M.A., El-Rabiei M.M., Nady H., Elgendy A., Zaki E.G., Abdou M.I. and Noamy E.S., Novel Ionic Liquid Compound Act as Sweet Corrosion Inhibitors for X-65 Carbon Tubing Steel: Experimental and Theoretical Studies. *Journal of Bio- and Tribo-Corrosion*, **3** (3), 31(2017).
27. Ibrahim M.N.M., Ahmed-Haras M.R., Sipaut C.S., Aboul-Enein H.Y. and Mohamed A.A., Preparation and characterization of a newly water soluble lignin graft copolymer from oil palm lignocellulosic waste. *Carbohydrate polymers*, **80** (4), 1102-1110 (2010).
28. El-Tabey A.S., Elsharaky E. and El-Tabey A.E., A Comparative the Inhibition Performance of a Newly Synthesized Cationic Surfmer and It's Oligomer Surfactant for Carbon Steel Corrosion in 1M Acid Chloride Solution. *INTERNATIONAL JOURNAL OF ELECTROCHEMICAL SCIENCE*, **11** (12), 10978-11001(2016).
29. Migahed M., Abd-El-Raouf M., Al-Sabagh A. and Abd-El-Bary H., Effectiveness of some non ionic surfactants as corrosion inhibitors for carbon steel pipelines in oil fields. *Electrochimica Acta*, **50** (24), 4683-4689 (2005).
30. Migahed M., Mohamed H. and Al-Sabagh A., Corrosion inhibition of H-11 type carbon steel in 1 M hydrochloric acid solution by N-propyl amino lauryl amide and its ethoxylated derivatives. *Materials chemistry and physics*, **80** (1), 169-175 (2003).
31. Chang K.-C., Chen S.-T., Lin H.-F., Lin C.-Y., Huang H.-H., Yeh J.-M. and Yu Y.-H., Effect of clay on the corrosion protection efficiency of PMMA/Na⁺-MMT clay nanocomposite coatings evaluated by electrochemical measurements. *European Polymer Journal*, **44** (1), 13-23(2008).
32. Migahed M.A., Hegazy M.A. and Al-Sabagh A.M., Synergistic inhibition effect between Cu²⁺ and cationic gemini surfactant on the corrosion of downhole tubing steel during secondary oil recovery of old wells. *Corrosion Science*, **61**, 10-18 (2012).
33. Al-Sabagh A.M., Nasser N.M., Farag A.A., Migahed M.A., Eissa A.M.F. and Mahmoud T., Structure effect of some amine derivatives on corrosion inhibition efficiency for carbon steel in acidic media using electrochemical and Quantum Theory Methods. *Egyptian Journal of Petroleum*, **22** (1), 101-116(2013).
34. Amin M.A., Weight loss, polarization, electrochemical impedance spectroscopy, SEM and EDX studies of the corrosion inhibition of copper in aerated NaCl solutions. *Journal of Applied Electrochemistry*, **36** (2), 215-226 (2006).
35. Amar H., Tounsi A., Makayssi A., Derja A., Benzakour J. and Outzourhit A., Corrosion inhibition of Armco iron by 2-mercaptobenzimidazole in sodium chloride 3% media. *Corrosion Science*, **49** (7), 2936-2945(2007).
36. Paria S. and Khilar K.C., A review on experimental studies of surfactant adsorption at the hydrophilic solid-water interface. *Advances in Colloid and Interface Science*, **110** (3), 75-95(2004).
37. Hernández R.d.P.B., Aoki I.V., Tribollet B. and de Melo H.G., Electrochemical impedance spectroscopy investigation of the electrochemical behaviour of copper coated with artificial patina layers and submitted to wet and dry cycles. *Electrochimica Acta*, **56** (7), 2801-2814(2011).
38. Tamilselvi S., Murugaraj R. and Rajendran N., Electrochemical impedance spectroscopic studies of titanium and its alloys in saline medium. *Materials and Corrosion*, **58** (2), 113-120(2007).
39. Ostovari A., Hoseinieh S.M., Peikari M., Shadzadeh S.R. and Hashemi S.J., Corrosion inhibition of mild steel in 1M HCl solution by henna extract: A comparative study of the inhibition by henna and its constituents (Lawson, Gallic acid, α -d-Glucose and Tannic acid). *Corrosion Science*, **51** (9), 1935-1949 (2009).
40. He Z. and Mansfeld F., Exploring the use of electrochemical impedance spectroscopy (EIS) in microbial fuel cell studies. *Energy & Environmental Science*, **2** (2), 215-219 (2009).
41. Rosliza R., Senin H.B. and Nik W.B.W., Electrochemical properties and corrosion inhibition of AA6061 in tropical seawater. *Colloids and Surfaces A: Physicochemical and Engineering Aspects*, **312**(2), 185-189(2008).
42. Al-Sabagh A.M., Migahed M.A., Sadeek S.A. and El Basiony N.M., Inhibition of mild steel corrosion and calcium sulfate formation in highly saline synthetic water by a newly synthesized anionic carboxylated surfactant. *Egyptian Journal of Petroleum*, **27** (4), 811-821 (2018).
43. Al-Sabagh A.M., El Basiony N.M., Sadeek S.A. and Migahed M.A., Scale and corrosion inhibition performance of the newly synthesized anionic

- surfactant in desalination plants: Experimental, and theoretical investigations. *Desalination*, **437**, 45-58(2018).
44. Al-Sabagh A.M., Nasser N.M., El-Azabawy O.E. and Tabey A.E.E., Corrosion inhibition behavior of new synthesized nonionic surfactants based on amino acid on carbon steel in acid media. *Journal of Molecular Liquids*, **219**, 1078-1088 (2016).
45. Zhang X.L., Jiang Z.H., Yao Z.P., Song Y. and Wu Z.D., Effects of scan rate on the potentiodynamic polarization curve obtained to determine the Tafel slopes and corrosion current density. *Corrosion Science*, **51** (3), 581-587 (2009).
46. Curioni M., The behaviour of magnesium during free corrosion and potentiodynamic polarization investigated by real-time hydrogen measurement and optical imaging. *Electrochimica Acta*, **120** 284-292 (2014).
47. Hassan H.H., Abdelghani E. and Amin M.A., Inhibition of mild steel corrosion in hydrochloric acid solution by triazole derivatives: Part I. Polarization and EIS studies. *Electrochimica Acta*, **52** (22), 6359-6366 (2007).
48. Ahamad I., Prasad R. and Quraishi M.A., Adsorption and inhibitive properties of some new Mannich bases of Isatin derivatives on corrosion of mild steel in acidic media. *Corrosion Science*, **52** (4), 1472-1481(2010).
49. Hill T.L., Emmett P.H. and Joyner L.G., Calculation of Thermodynamic Functions of Adsorbed Molecules from Adsorption Isotherm Measurements: Nitrogen on Graphon 1,2. *Journal of the American Chemical Society*, **73** (11), 5102-5107 (1951).
50. Christov M. and Popova A., Adsorption characteristics of corrosion inhibitors from corrosion rate measurements. *Corrosion Science*, **46** (7), 1613-1620 (2004).
51. El Basiony N.M., Elgendy A., Nady H., Migahed M.A. and Zaki E.G., Adsorption characteristics and inhibition effect of two Schiff base compounds on corrosion of mild steel in 0.5 M HCl solution: experimental, DFT studies, and Monte Carlo simulation. *RSC Advances*, **9** (19), 10473-10485 (2019).
52. Migahed M.A., Mohamed H.M. and Al-Sabagh A.M., Corrosion inhibition of H-11 type carbon steel in 1 M hydrochloric acid solution by N-propyl amino lauryl amide and its ethoxylated derivatives. *Materials Chemistry and Physics*, **80** (1), 169-175 (2003).
53. Al-Sabagh A.M., Abd-El-Bary H.M., El-Ghazawy R.A., Mishrif M.R. and Hussein B.M., Corrosion inhibition efficiency of heavy alkyl benzene derivatives for carbon steel pipelines in 1M HCl. *Egyptian Journal of Petroleum*, **21**(2), 89-100 (2012).
54. Abd-Elaal A.A., Elbasiony N.M., Shaban S.M. and Zaki E.G., Studying the corrosion inhibition of some prepared nonionic surfactants based on 3-(4-hydroxyphenyl) propanoic acid and estimating the influence of silver nanoparticles on the surface parameters. *Journal of Molecular Liquids*, **249**, 304-317 (2018).
55. Migahed M.A., Elgendy A., El-Rabiei M.M., Nady H. and Zaki E.G., Novel Gemini cationic surfactants as anti-corrosion for X-65 steel dissolution in oilfield produced water under sweet conditions: Combined experimental and computational investigations. *Journal of Molecular Structure*, **1159**, 10-22(2018).

تحضير وتقييم بعض البوليمرات الكاتيونية الجديدة ذات النشاط السطحي لإستخدامها كمواد مثبطة لتآكل الصلب الكربوني في مياة تكوين الآبار

أميرة التابعى^١، احمد جمال بدير^١، إيمان خميس^١، محمد عبدالرؤف^١، فواد زهران^٢، عادل يوسف^٢، احمد الصباغ^٣
^١معهد بحوث البترول - مدينة نصر- القاهرة - مصر.
^٢كلية العلوم - جامعة حلوان - حلوان - القاهرة - مصر.
^٣مركز النانوتكنولوجي - جامعة حلوان - القاهرة؛ مصر.

تتميز البوليمرات الكاتيونية ذات النشاط السطحي بقدرتها على الإدمصاص على سطح الصلب الكربوني مكونة طبقة رقيقة تحمية من التآكل من مياة تكوين الآبار الناتجة عن استخراج المواد البترولية.

لذا تم تحضير بوليمرات كاتيونية تم تسميتها PTEAA.10 & PTEAA.12 بالخطوات التالية:

١. تحضير أحادي الأستر عن طريق تفاعل حمض الأكريليك مع ثلاثي إيثانول الأمين ثم بلمرة الأستر المتكون.
٢. تفاعل البوليمر الناتج من الخطوة السابقة مع هاليدات الألكيل ذات السلاسل الكربونية المختلفة للحصول على بوليمرات كاتيونية.

وقد تم إثبات التركيب الكيميائي للبوليمرات المحضرة عن طريق FT-IR و ¹H-NMR و ¹³C-NMR وتعيين الوزن الجزيئي بإستخدام كروماتوجرافيا تعتمد على نفاذية الهلام. علاوة على ذلك تم دراسة تأثير البوليمرات الكاتيونية المحضرة كمشببات للتآكل للصلب الكربوني في مياة تكوين الآبار بالطرق التالية:

- طريقة فقد الوزن.
- مقاومة الاستقطاب.
- الممانعة الكهروكيميائية.

وتبين من ذلك فاعلية البوليمرات الكاتيونية كمواد مثبطة للتآكل وتزداد الكفاءة بزيادة طول السلسلة الكربونية الغير محبة للماء محققة نسبة حماية من التآكل للصلب الكربوني تجاوزت ٩٢ ٪ وتبين ذلك بوضوح من دراسة شكل السطح عن طريق الماسح بالمجهر الإلكتروني.